



TITLE:

# Near-infrared spectroscopy as a potential method for identification of anatomically similar Japanese diploxylons

AUTHOR(S):

Horikawa, Yoshiki; Mizuno-Tazuru, Suyako;  
Sugiyama, Junji

---

CITATION:

Horikawa, Yoshiki ...[et al]. Near-infrared spectroscopy as a potential method for identification of anatomically similar Japanese diploxylons. Journal of Wood Science 2015, 61(3): 251-261

ISSUE DATE:

2015-01-31

URL:

<http://hdl.handle.net/2433/201492>

RIGHT:

The final publication is available at Springer via <http://dx.doi.org/10.1007/s10086-015-1462-2>; The full-text file will be made open to the public on 31 January 2016 in accordance with publisher's 'Terms and Conditions for Self-Archiving'; This is not the published version. Please cite only the published version.; この論文は出版社版ではありません。引用の際には出版社版をご確認ご利用ください。

1    **Near-infrared spectroscopy as a potential method for identification of anatomically**  
2    **similar Japanese diploxylons**

3  
4    Yoshiki Horikawa<sup>\*</sup>, Suyako (Mizuno) Tazuru, Junji Sugiyama

5  
6    Research Institute for Sustainable Humanosphere, Kyoto University, Kyoto, Japan

7  
8  
9    <sup>\*</sup>Tel: +81-774-38-3634

10   Fax: +81-774-38-3635

11   E-mail: yhorikawa@rish.kyoto-u.ac.jp

12  
13   **Keywords:** Discriminant analysis; NIR spectroscopy; Japanese diploxylons; Wood  
14   identification; Aging wood

15

16

17

18

19

20    **Abstract**

21            A reliable technique for distinguishing anatomically similar dipoxylons, *Pinus*  
22    *densiflora* and *P. thunbergii*, was designed by employing near-infrared (NIR) spectroscopy in  
23    combination with multivariate analysis. In total, 24 wood blocks, with half of them being of *P.*  
24    *densiflora* and the rest of *P. thunbergii*, were selected from the collections of the Kyoto  
25    University xylarium and scrutinized to build an acceptable model for discriminating between  
26    the two species. The prediction model was constructed only from heartwood, and the best  
27    performance was obtained for wavenumbers of 7300–4000 cm<sup>-1</sup> in the second derivative  
28    spectra. To apply this model to actual materials obtained from historical wooden buildings, 12  
29    aging wood samples were analyzed and compared by microscopic identification.  
30    Unexpectedly, the spectral differences between the species were smaller than those caused by  
31    aging, and the prediction error was approximately 50%. The spectra of the aging samples  
32    were quite distinct in the specific region characteristic of absorbed water (5220 cm<sup>-1</sup>); this  
33    was demonstrated clearly by principal component analysis. Therefore, for the proposed  
34    model to be suitable for use in practical applications, further investigations of aging wood  
35    samples and the corresponding spectroscopic data are necessary in order to understand the  
36    effects of aging on the spectral data.

37

## 38 Introduction

39 *Pinus densiflora* and *P. thunbergii* are varieties of pine trees that are very popular in  
40 Japan. The former is known as akamatsu and mematsu, and the latter as kuromatsu and  
41 omatsu. Both are planted widely in Japan for timber production and as ornamental trees and  
42 are a characteristic feature of classical Japanese gardens. *P. densiflora* is commonly seen  
43 growing on the low mountains and hillsides, while *P. thunbergii* is native to the coastal areas.

44 Anatomically, the two species are nearly identical in terms of the resin canal, which  
45 is surrounded by thin-walled epithelial cells and window-type cross-field pitting and exhibits  
46 a distinct transition from earlywood to latewood. The key difference between the two species  
47 was reported to be the degree of dentate thickening of the ray tracheids (Fig. 1). However,  
48 this difference is rather subjective and can be misleading, particularly in old samples, whose  
49 cell walls have nearly deteriorated. Consequently, in many previous studies, these pine wood  
50 species have been identified simply as diploxylons and their particular species has been left  
51 undecided. Therefore, an alternative method that could allow for the identification of the  
52 particular species without requiring special experimentation would be highly desirable.

53 In this regard, near-infrared (NIR) spectroscopy, which is known as a rapid, accurate  
54 and reproducible analysis technique, is an attractive choice. NIR spectroscopy is also suitable  
55 for assessing wood materials because the bands attributable to the vibrations of the chemical  
56 bonds involved in the formation of the cell wall allow for the direct and indirect estimation of



the chemical and physical properties of the materials. When combined with multivariate analysis, NIR spectroscopy can be used to distinguish between different wood species. Schimleck et al. demonstrated that principal component analysis (PCA) could be used to distinguish between pine and eucalyptus and also to differentiate between samples of the same eucalyptus species grown at different sites [1]. Soft independent modeling of class analogy has also been used to classify wood samples, including red and white oak [2] and larch species [3]. Regression analysis, especially partial least square (PLS) regression, is a powerful method of accurately estimating the chemical compositions of wood samples [4] and of determining their enzymatic hydrolysis [5] and decay resistance [6], in addition to their physical properties, such as fiber length [7-9], cellulose microfibril angle [10], and stiffness [11]. The method of distinguishing species coupled with regression analysis, called partial least squares-discriminant analysis (PLS-DA), has been used as a tool for differentiating true mahogany from three other similar species [12, 13]. Sandberg and Sterley [14] could successfully distinguish between heartwood and sapwood samples of Norway spruce using the PLS algorithm. Watanabe et al. [15] could differentiate between aging and degraded samples of softwood, such as *Chamaecyparis obtusa*, *Torreya nucifera*, and *C. pisifera* using PLS.

In this study, we first describe a simple technique that uses NIR spectroscopy in combination with PLS-DA for distinguishing *P. densiflora* from *P. thunbergii*, which were

classified at the xylarium of Kyoto University. The discriminant model was initially examined using complete sets of the wood samples. Later, the sapwood and heartwood samples were analyzed separately. Next, we demonstrate the applicability of the proposed method in determining the species of aging samples of wood, and discuss the factors that influence the precision of discrimination.

## Materials and methods

### Sampling

Wood blocks of *P. densiflora* designated as KYOw00029, 00225, 08058, 08059, 09268, 13942, 19360, and 19361, and those of *P. thunbergii* designated as KYOw00030, 00520, 05509, 05639, 08071, 10321, 11386, 13913, and 19176 by the xylarium at the Research Institute for Sustainable Humansphere, Kyoto University (<http://database.rish.kyoto-u.ac.jp/cgi-bin/bmi/en/namazu.cgi>) were used for establishing the discriminant model. The wood samples in these blocks were collected from all the sapwood and heartwood zones. However, in the case of the wood blocks of KYOw00029, 05639, 08071, 09268, and 13913, only sapwood was collected. On the other hand, only heartwood was taken from KYOw00520, 19176, 19360, and 19361. Three parts were collected randomly from each wood block after NIR spectral analysis. Finally, wood samples from Chion-In temple in Kyoto, Japan and designated as KYO\_ID\_5165, 5166, 5168, 5170, 5173, 5175, 5185, 5187, 5189, 5192, 5197, and 5252 [16] were used to test applicability of the

95 proposed method. Blocks were collected from each of these aging samples.

## 96 **Optical microscopy**

97 In the case of the wood samples obtained from the xylarium for the construction of  
98 the calibration model, radial sections approximately 30  $\mu\text{m}$  in thickness were cut using a  
99 sliding microtome and were stained with safranin. In the case of the wood samples from  
100 Chion-in, the corresponding sections were obtained by hand sectioning and were not stained.  
101 The sections were observed using a light microscope (Olympus BX51) equipped with a  
102 digital camera (Olympus DP73).

## 103 **NIR spectroscopy**

104 Each wood block after air-drying was milled with a rough file to produce a powder  
105 sample. Then, a tablet was prepared by collecting approximately 0.04 g of the powder, which  
106 was hand pressed following a previously published protocol [17]. The NIR spectrum was  
107 obtained using a PerkinElmer Spectrum 100N system for wavenumbers of 10000–4000  $\text{cm}^{-1}$   
108 at a spectral resolution of 16  $\text{cm}^{-1}$ ; 32 scans were made for each sample. The prepared tablet  
109 was placed directly on the NIR integrating sphere diffuse reflectance accessory (PerkinElmer),  
110 which had a triglycine sulfate detector. Both faces of each tablet were scanned. The  
111 absorbance spectrum was recorded by normalizing the single-beam spectrum against the  
112 background spectrum using a Teflon-based material (Spectralon; LabSphere, North Sutton,  
113 NH). The original spectrum was treated using the Savitzky–Golay second derivative [18]

using 9 points and a fifth-order polynomial for the smoothing before the multivariate analysis.

## Multivariate analysis

PLS-DA and PCA were performed using a commercial software (Unscrambler v.9.8; CAMO Software, Inc., Woodbridge, NJ). Calibration and prediction samples from the 144 spectra (72 each for the sapwood and heartwood samples) were randomly selected as the ratio at 2 to 1, that is, 96 were used for calibration, and 48 were used for the prediction set. Of the spectra used for calibration, 48 belonged to *P. densiflora* and 48 belonged to *P. thunbergii*. In the case of the spectra used for prediction, 24 belonged to *P. densiflora* and 24 belonged to *P. thunbergii*, as shown in Table 1. For the development of a discriminant model for use in the multivariate analysis, we assigned *P. densiflora* a class value of +1 and *P. thunbergii* a class value of -1 in the calibration set. The PLS factors were determined by cross validation; a single sample was kept out of the model, and its characteristics were predicted by constructing a model without the sample. Excessively high numbers may result in overfitting; therefore, the number of PLS factors was kept at fewer than 11. The coefficient of determination for calibration ( $R_c^2$ ) and the root mean square error of calibration (RMSEC) were used to assess the calibration performance. The models developed were evaluated by using the coefficient of determination of prediction ( $R_p^2$ ) and the root mean square error of prediction (RMSEP). The percentage of correct prediction was determined as the proportion

of the number of species discriminated correctly compared to the total number of samples from prediction set. PLS-DA to distinguish between sapwood and heartwood was also performed using the same procedure.

PCA was performed on the basis of the second derivative spectra of all the wood samples for wavenumbers of 7300–4000  $\text{cm}^{-1}$ . The PC loading was obtained from the model built for score plots.

## Results and Discussion

### Discriminant model for determining the type of wood present

Fig. 2a and b show original and second derivative spectra from heart and sapwood samples of *P. densiflora* and *P. thunbergii*. From the band at 5220  $\text{cm}^{-1}$  assigned to absorbed water in second derivative NIR spectra, sapwood samples seemed higher moisture contents than those of heartwood. However, it was difficult to identify whether *P. densiflora* or *P. thunbergii* from spectra because spectral pattern including the bands at 5980 and 5800  $\text{cm}^{-1}$  specific to lignin and hemicellulose respectively, were almost same between these species. Therefore, we applied multivariate analysis and Table 2 shows the statistical summary of the discriminant models obtained on the basis of the original spectra and the second derivative spectra. To generate a better model, the regions of the NIR spectra corresponding to the wavenumbers of 10000–4000  $\text{cm}^{-1}$  were separated into four distinct ranges on the basis of the properties of the molecular vibrations. In the first range (10000–7300  $\text{cm}^{-1}$ ), the second or

third overtones were involved, although less information was obtained from the wood samples. The second range (7300–6050  $\text{cm}^{-1}$ ) mainly corresponded to OH overtone vibrations. The third range (6050–5500  $\text{cm}^{-1}$ ) corresponded to the CH vibrations and the vibrations from the aromatic framework, while in the fourth range (5500–4000  $\text{cm}^{-1}$ ), several combinatorial vibrations were present.

For the samples containing both sapwood and heartwood, the discriminant models shown in Table 2a were constructed on the basis of the NIR spectra without subjecting the spectra to any spectral pretreatment. All the models were unreliable because the  $R_p^2$  values were less than 0.60. Next, we obtained the second derivative spectra and created the discriminant models shown in Table 2b. Secondary differentiation can extract information hidden in the original spectra. Thus, researchers have often applied this algorithm to construct regression models. This spectral pretreatment decreased the number of factors relatively; however, the models obtained were not markedly better. Fig. 3a shows a histogram corresponding to the discriminant model based on the second derivative spectra for 7300–4000  $\text{cm}^{-1}$ . In this region, a few samples of both *P. densiflora* and *P. thunbergii* had class values of approximately 0, which indicated that this model could not be used for distinguishing between the two species.

Sapwood could, therefore, be distinguished from heartwood, and discriminant models could be built, as summarized in Tables 2c and d. However, as was the case with the

dataset corresponding to the samples containing both sapwood and heartwood, all the models showed poor performances, as the  $R_p^2$  values were lower than 0.75. Fig. 3b shows a histogram based on the second derivative spectra for 7300–4000  $\text{cm}^{-1}$ ; for this region, the RMSEP value was 0.54 and the  $R_p^2$  value was 0.71, with some of the prediction samples from *P. thunbergii* having class values of 0 and similar to those of *P. densiflora*.

In the case of heartwood, even though a large number of factors were required, the calibration performance was comparatively better (Table 2e). However, the models obtained using the vibrations over 10000–7300  $\text{cm}^{-1}$  and 7300–6050  $\text{cm}^{-1}$  were less reliable; this was particularly true in the latter case, where the major bands were assigned to cellulose [19-21]. This suggested that the cellulose contents were indistinct between *P. densiflora* and *P. thunbergii* as well as their crystalline properties.

The discriminant models obtained using the second derivative spectra are shown in Table 2f. The models exhibited better performances as the  $R_p^2$  values corresponding to a few of the NIR spectral regions were higher than 0.85. The best performance was obtained for 7300–4000  $\text{cm}^{-1}$ ; this region showed an RMSEP value of 0.37,  $R_p^2$  value of 0.86 and 100 % accuracy of identification. As shown in Fig. 3c, the prediction model based on the corresponding region allowed us to classify all the samples from *P. densiflora* as having positive values, while the samples for classifying *P. thunbergii* were placed in another group and had negative values.

NIR spectroscopy is sensitive to the functional groups and is thus influenced by the chemical and structural features of the cell walls of the trees being investigated. Therefore, the difficulties encountered in classification using sapwood samples indicated that the chemical natures of *P. densiflora* and *P. thunbergii* were essentially indistinct. However, the fact that using heartwood samples yielded better results suggested that the heartwood components of the two species might be slightly different.

### **Applicability in investigating aging wood used in traditional buildings**

The applicability of the regression model developed was tested by reexamining actual wood materials used in traditional wooden buildings built in the medieval period. Chion-In temple in Kyoto is well known and is the main temple of Jōdo Shū ("The Pure Land School"). The wood materials used in the Shūedō (i.e., the Assembly Hall) had been studied during 2005–2010, and 25 wood samples had been classified as being of diploxylons [16]. Twelve specimens were used in the present study. The enlarged radial sections of the ray tracheids of these samples are shown in Fig. 4. Of these 12 samples, only three were anatomically identified as *P. thunbergii* on the basis of the degree of dentate thickening in the ray tracheids. The PLS-DA models built up on the basis of heartwood were used in the identification of these materials. The percentage of coincidence with the anatomical identification results is listed in Table 3. In contrast to the prediction set samples shown in Tables 2e and f, the discriminant models failed to predict the species perfectly. One possible



209 reason behind this failure seems to be the fact that the wood used in Chion-in was sapwood,  
210 while the calibration models used for identification were created using heartwood. However,  
211 sapwood is usually not used as a building material, in order to minimize deterioration and  
212 maintain the structural strength. Given this background, we investigated these aging wood  
213 samples further using NIR spectroscopy in combination with multivariate analysis, as  
214 mentioned in the next segment.

## 215 **Effects of aging**

216 To understand the reason for the failure in prediction of Chion-in materials, PCA was  
217 carried out in the wavenumber range  $7300\text{--}4000\text{ cm}^{-1}$  of the second derivative spectra (Fig.  
218 5a). The score plots showed that some of the wood samples from Chion-In temple localized  
219 on the left side and far from those belonging to *P. densiflora* and *P. thunbergii*. It is known  
220 that noncrystalline polysaccharides such as hemicellulose decrease in quantity in aging  
221 samples of *C. obtusa*, whereas the crystalline cellulose region is not affected [22].  
222 Furthermore, Yokoyama et al. reported that the equilibrium moisture content in *C. obtusa*  
223 decreases after aging [23]. Therefore, it seems that aging under dry conditions degraded the  
224 hemicelluloses, which are the adsorption sites for water in wood materials, resulting in a  
225 decrease in the equilibrium moisture content. In this regard, the wood samples from Chion-in  
226 temple were different in that there was no statistical difference between modern and aging  
227 woods in hemicellulose contents, given the presence of the band at approximately  $5800\text{ cm}^{-1}$ ;

228 this band is specific to furanose/pyranose, which form from hemicellulose [24] and exhibited  
229 a value of almost 0 in the PC1 loading (Fig. 5b). In addition, the amount of absorbed water in  
230 the Chion-in samples was higher, as a positive band was noticed at approximately  $5220\text{ cm}^{-1}$   
231 and was assignable to the combinational vibration of water; this was clearly visible in the  
232 PC1 loading. Moreover, the lignin content of the Chion-in samples was lower, as a band was  
233 noticed at  $5970\text{ cm}^{-1}$ ; this band is characteristic of aromatic skeletal vibrations [24] and  
234 exhibited negative values during PC1 loading. These interpretation was supported by the  
235 comparison with the second derivative spectra between modern and aging wood (Fig. 5c).  
236 Therefore, the lignin in the Chion-in samples seemed to be modified to a greater degree than  
237 was the hemicellulose, which resulted in a decrease in the hydrophobicity, as this increased  
238 the amount of absorbed water. These features were not observed in the spectra of the unaging  
239 wood samples. Hence, the samples from Chion-in could not be classified accurately. In order  
240 to be able to employ the proposed classification method for identifying historical and  
241 archeological wood samples, we have to consider the effects of aging on the characteristics of  
242 the samples, including on the quantity of absorbed water and the chemical components such  
243 as lignin and polysaccharides, whose chemical structure can be changed by oxidative and/or  
244 enzymatic reactions. Therefore, further investigations need to be performed to determine the  
245 optimal conditions for measurements as well as suitable data treatments to account for the  
246 spectral variations caused by aging, in order to be able to distinguish between *P. densiflora*

247 and *P. thunbergii* on the basis of the differences in their spectra.

## 248 **Conclusions**

249 When using unaging heartwood samples, we were able to identify *P. densiflora* and *P.*  
250 *thunbergii* by employing NIR spectroscopy in combination with multivariate analysis.  
251 However, when aging wood samples were used, the proposed method was ineffective in  
252 distinguishing between the two species. Thus, the method is not suitable for classifying wood  
253 samples from historical and archeological buildings. However, further research is underway  
254 to find the spectral features between these microscopically similar species more significant  
255 than those caused by aging.

256

## 257 **Acknowledgments**

258 The study was supported in parts by Grants-in-Aid for Scientific Research (Grant Numbers  
259 25252033, 22300309, and 24780169) from the Japan Society for the Promotion of Science  
260 (JSPS). The authors thank Ms. Izumi Kanai and Mr. Akio Adachi for their technical support.

## 261 **References**

- 262 [1] Schimleck LR, Evans R, Ilic J, Matheson AC (2002) Estimation of wood stiffness of  
263 increment cores by near-infrared spectroscopy. Can J For Res 32: 129–135
- 264 [2] Adedipe OE, Dawson-Andoh B, Slahor J, Osborn L (2008) Classification of red oak  
265 (*Quercus rubra*) and white oak (*Quercus alba*) wood using a near infrared spectrometer and  
266 soft independent modelling of class analogies. J Near Infrared Spectrosc 16: 49–57

- 267 [3] Gierlinger N, Schwanninger M, Wimmer R (2004) Characteristics and classification  
268 of Fourier-transform near infrared spectra of the heartwood of different larch species (*Larix*  
269 sp.). J Near Infrared Spectrosc 12: 113–119
- 270 [4] Jones PD, Schimleck LR, Peter GF, Daniels RF, Clark A (2006) Nondestructive  
271 estimation of wood chemical composition of sections of radial wood strips by diffuse  
272 reflectance near infrared spectroscopy. Wood Sci Technol 40: 709–720
- 273 [5] Horikawa Y, Imai T, Takada R, Watanabe T, Takabe K, Kobayashi Y, Sugiyama J  
274 (2012) Chemometric analysis with near-infrared spectroscopy for chemically pretreated  
275 Erianthus toward efficient bioethanol production. Appl Biochem Biotechnol 166: 711–721
- 276 [6] Leinonen A, Harju AM, Venalainen M, Saranpaa P, Laakso T (2008) FT-NIR  
277 spectroscopy in predicting the decay resistance related characteristics of solid Scots pine  
278 (*Pinus sylvestris* L.) heartwood. Holzforschung 62: 284–288
- 279 [7] Hauksson JB, Bergqvist G, Bergsten U, Sjostrom M, Edlund U (2001) Prediction of  
280 basic wood properties for Norway spruce. Interpretation of near infrared spectroscopy data  
281 using partial least squares regression. Wood Sci Technol 35: 475–485
- 282 [8] Inagaki T, Schwanninger M, Kato R, Kurata Y, Thanapase W, Puthson P,  
283 Tsuchikawa S (2010) *Eucalyptus camaldulensis* density and fiber length estimated by  
284 near-infrared spectroscopy. Wood Sci Technol 46: 143–155
- 285 [9] Schimleck LR, Jones RD, Peter GF, Daniels RF, Clark A (2004) Nondestructive

- 286 estimation of tracheid length from sections of radial wood strips by near infrared  
287 spectroscopy. *Holzforschung* 58: 375–381
- 288 [10] Schimleck LR, Evans R, Jones PD, Daniels RF, Peter GF, Clark A (2005)  
289 Estimation of microfibril angle and stiffness by near infrared spectroscopy using sample sets  
290 having limited wood density variation. *IAWA J* 26: 175–187
- 291 [11] Schimleck LR, Michell AJ, Vinden P (1996) Eucalypt wood classification by NIR  
292 spectroscopy and principal components analysis. *Appita J* 49: 319–324
- 293 [12] Braga JWB, Pastore TCM, Coradin VTR, Camargos JAA, da Silva AR (2011) The  
294 use of near infrared spectroscopy to identify solid wood specimens of *Swietenia Macrophylla*  
295 (Cites Appendix II). *IAWA J* 32: 285–296
- 296 [13] Pastore TCM, Braga JWB, Coradin VTR, Magalhaes WLE, Okino EYA, Camargos  
297 JAA, de Muniz GIB, Bressan OA, Davrieux F (2011) Near infrared spectroscopy (NIRS) as a  
298 potential tool for monitoring trade of similar woods: Discrimination of true mahogany, cedar,  
299 andiroba, and curupixa. *Holzforschung* 65: 73–80
- 300 [14] Sandberg K, Sterley M (2009) Separating Norway spruce heartwood and sapwood in  
301 dried condition with near-infrared spectroscopy and multivariate data analysis. *Eur J For Res*  
302 128: 475–481
- 303 [15] Watanabe K, Abe H, Kataoka Y, Nodhito S (2011) Species separation of aging and  
304 degraded solid wood using near infrared spectroscopy. *Jpn J Histor Bot* 19: 117–124

- 305 [16] Mizuno S, Sugiyama J (2011) Wood identification of building components of  
306 Syue-do, Chion-in temple designated as nationally important cultural property. *J Soc*  
307 *Architect Hits Japan* 56: 124–135
- 308 [17] Horikawa Y, Imai T, Takada R, Watanabe T, Takabe K, Kobayashi Y, Sugiyama J  
309 (2011) Near-infrared chemometric approach to exhaustive analysis of rice straw pretreated  
310 for bioethanol conversion. *Appl Biochem Biotechnol* 164: 194–203
- 311 [18] Savitzky A, Golay MJE (1964) Smoothing and differentiation of data by simplified  
312 least squares procedures. *Anal Chem* 36: 1627–1639
- 313 [19] Tsuchikawa S, Siesler HW (2003a) Near-infrared spectroscopic monitoring of the  
314 diffusion process of deuterium-labeled molecules in wood. Part I: Softwood. *Appl Spectrosc*  
315 57: 667–674
- 316 [20] Tsuchikawa S, Siesler HW (2003b) Near-infrared spectroscopic monitoring of the  
317 diffusion process of deuterium-labeled molecules in wood. Part II: Hardwood. *Appl*  
318 *Spectrosc.* 57: 675–681
- 319 [21] Watanabe A, Morita S, Ozaki Y (2006) A study on water adsorption onto  
320 microcrystalline cellulose by near-infrared spectroscopy with two-dimensional correlation  
321 spectroscopy and principal component analysis. *Appl Spectrosc* 60: 1054–1061
- 322 [22] Tsuchikawa S, Yonenobu H, Siesler HW (2005) Near-infrared spectroscopic  
323 observation of the ageing process in archaeological wood using a deuterium exchange

324 method. Analyst 130: 379–384

325 [23] Yokoyama M, Gril J, Matsuo M, Yano H, Sugiyama J, Clair B, Kubodera S,

326 Mitsutani T, Sakamoto M, Ozaki H, Imamura M, Kawai S (2009) Mechanical characteristics

327 of aged Hinoki wood from Japanese historical buildings. C R Physique 10: 601–611

328 [24] Siesler HW, Ozaki Y, Kawata S, Heise HW Near-infrared Spectroscopy, Principal

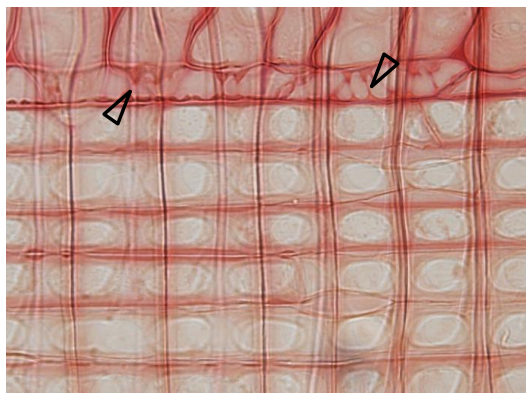
329 Instruments, Applications; Willey-VCH Verlag GmbH, Weinheim, Germany, 2002

330

331 Figures

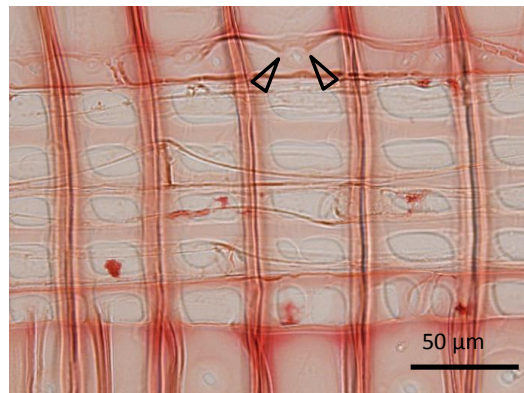
332

(a)



333

(b)



334 Fig. 1

335



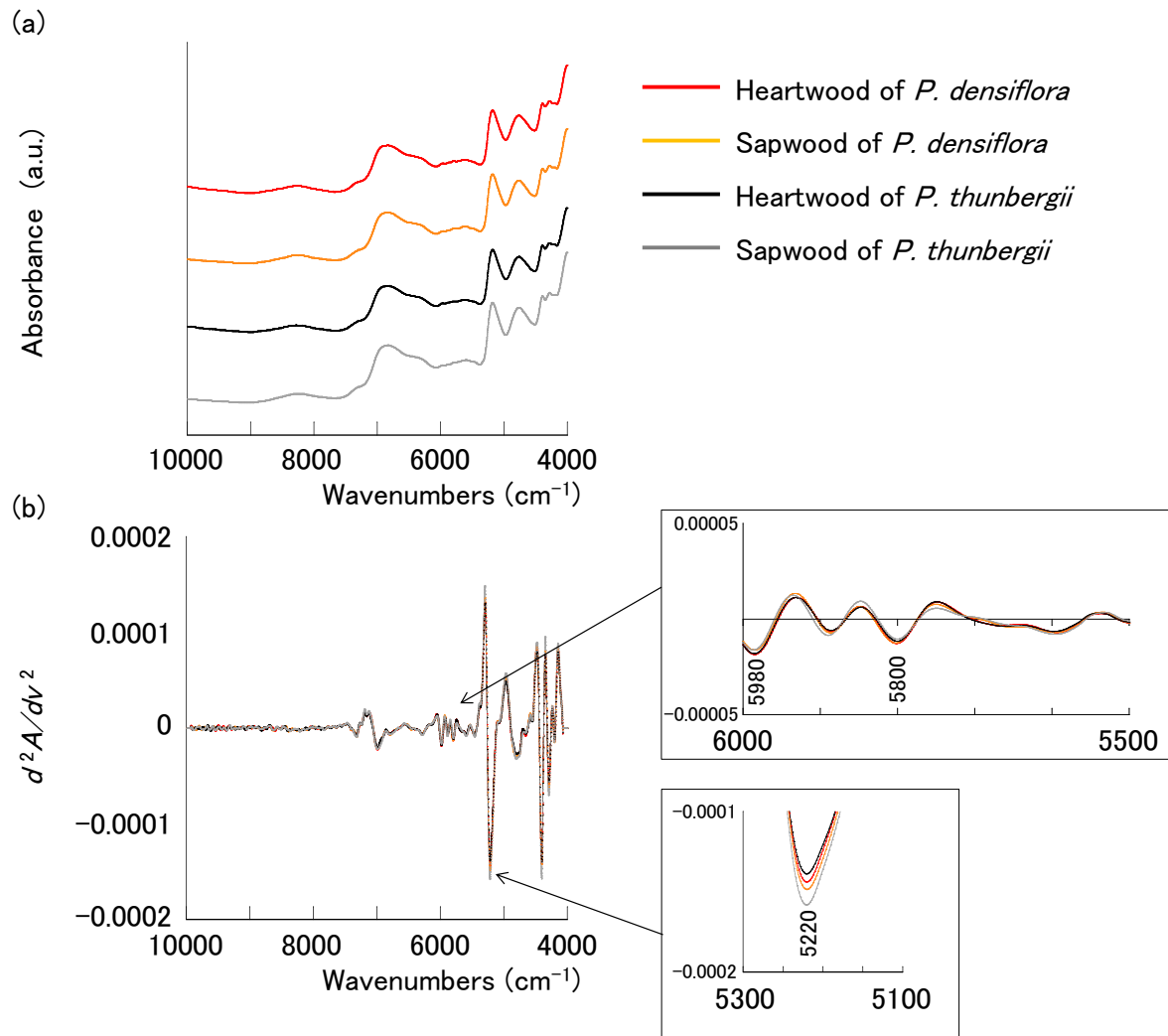


Fig. 2

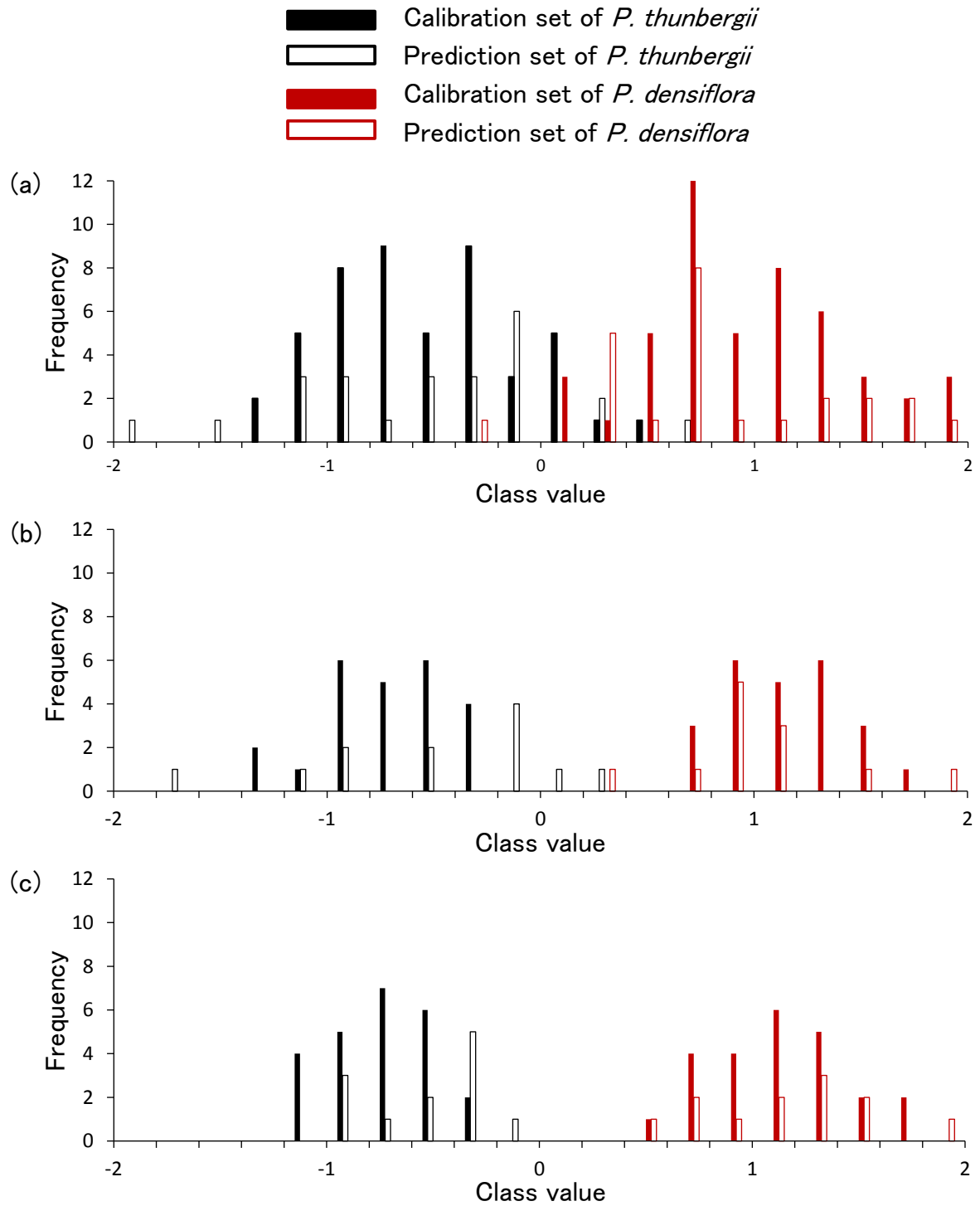
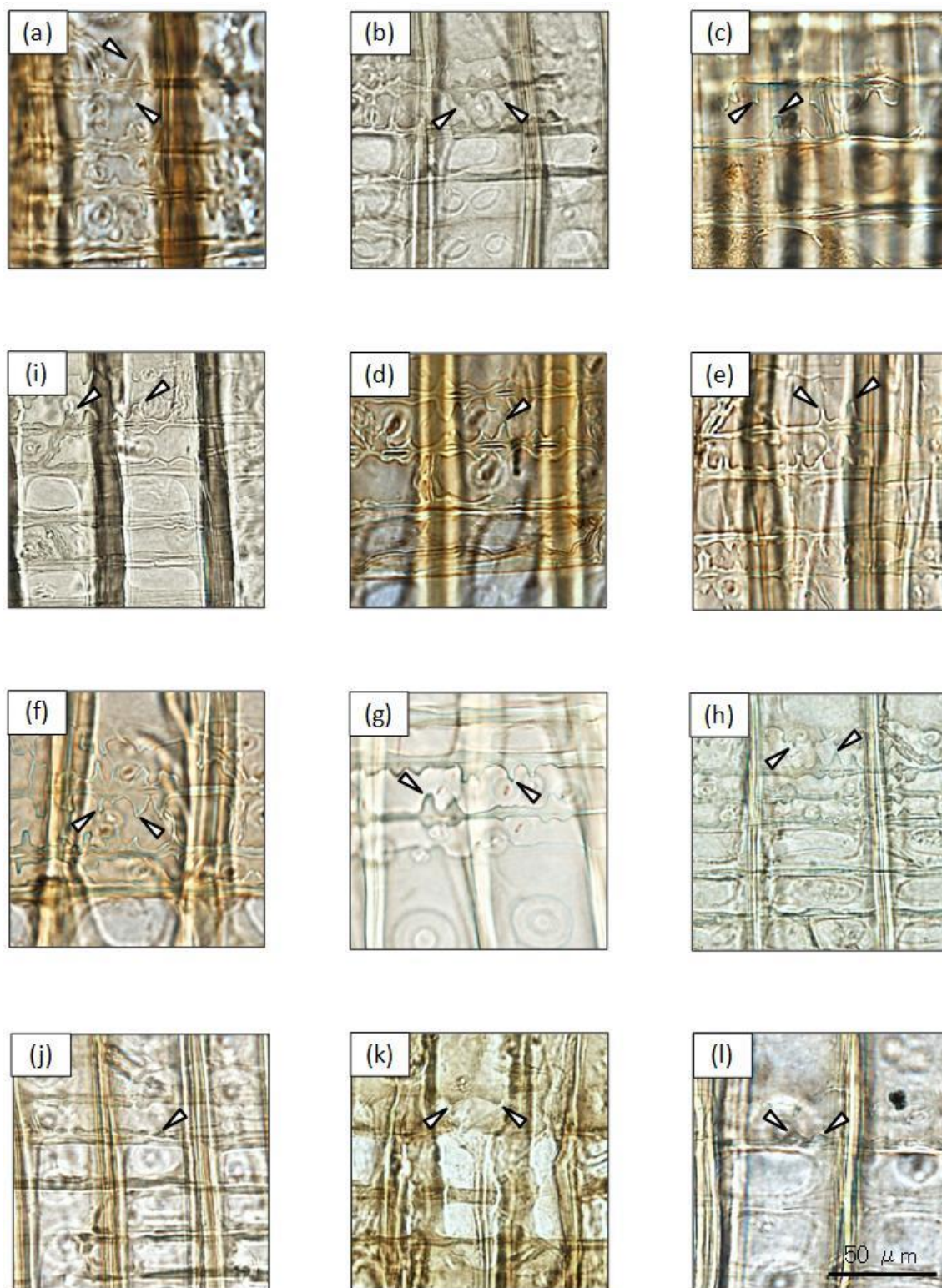


Fig. 3



347

348 Fig. 4

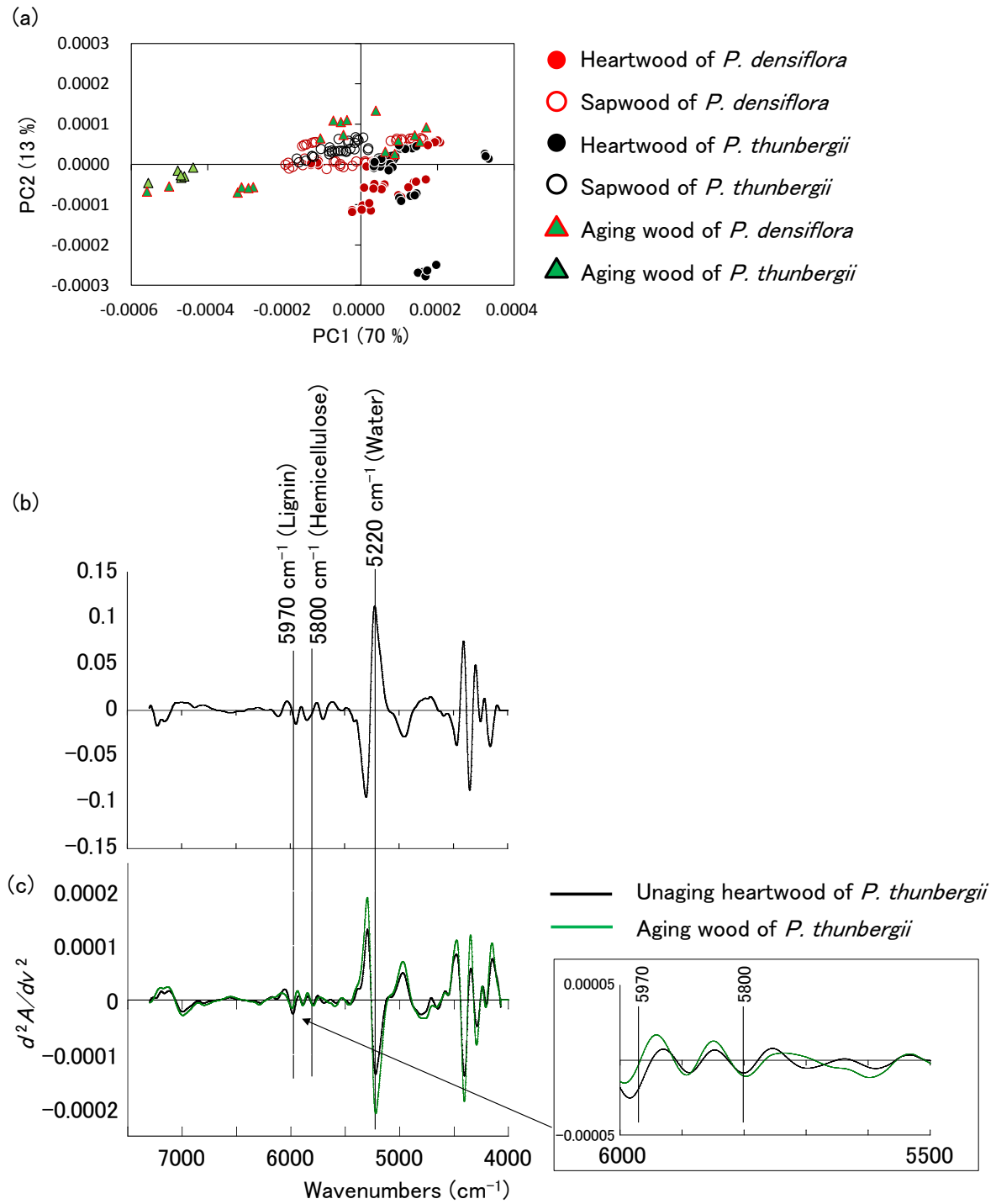


Fig. 5

## Figure legends

Fig. 1. Optical micrographs of the standard radial section. (a) *P. densiflora* shows dentate thickening within the ray tracheid, while (b) these features are smooth in *P. thunbergii*. The arrow heads indicate dentate thickening.

Fig. 2. (a) Original NIR spectra of heartwood and sapwood from *P. densiflora* and *P. thunbergii* designated as KYOw13942 and 00030, which were included in calibration set. (b) Second derivative spectra obtained from the 4 spectra in (a).

Fig. 3. Histograms of the class values computed by PLS-DA on the basis of the second derivative spectra for wavenumbers of 7300–4000  $\text{cm}^{-1}$  and obtained from (a) a mixture of sapwood and heartwood, (b) sapwood, and (c) heartwood.

Fig. 4. Optical micrographs of the radial sections acquired from wood samples from Chion-In temple. The images in (a)–(i) correspond to KYO\_ID\_5165, 5166, 5168, 5170, 5173, 5175, 5185, 5189, and 5252, respectively, which were identified as being of *P. densiflora*. The images in (j)–(l), which were acquired from KYO\_ID\_5187, 5192, and 5197, respectively, were identified as being of *P. thunbergii*. The arrow heads indicate dentate thickening.

371 Fig. 5. (a) The principal components analysis (PCA) scores plotted on the first and second  
372 principal components on the basis of the second derivative NIR spectra in the 7300–4000  
373  $\text{cm}^{-1}$  region.

374 (b) The spectrum obtained from PC1 loading in PCA. The bands at 5970, 5800, and 5220  
375  $\text{cm}^{-1}$  are assigned to lignin, hemicellulose, and the absorbed water, respectively.

376 (c) Second derivative spectra obtained from unaging heartwood and aging wood of *P.*  
377 *thunbergii* designated as KYOw19176 and KYO\_ID\_5197.

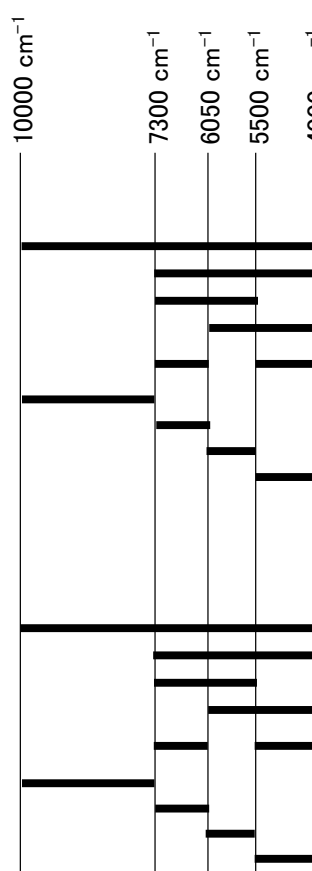
378

379

Table 1. The number of NIR spectra of the wood samples used for calibration and prediction.

		Calibration set	Prediction set	Total
<i>P. densiflora</i>	Sapwood	24	12	36
	Heartwood	24	12	36
<i>P. thunbergii</i>	Sapwood	24	12	36
	Heartwood	24	12	36
Total		96	48	144

Table 2. Statistical summary of the discriminant models based on the calibration and prediction sets obtained from a mixture of sapwood and heartwood samples (a and b), and individual sapwood (c and d) and heartwood (e and f) samples. The discriminant models were obtained by using the original spectra (a, c and e) and the second derivative spectra (b, d and f). A schematic illustration is shown on the left to indicate each spectral region.



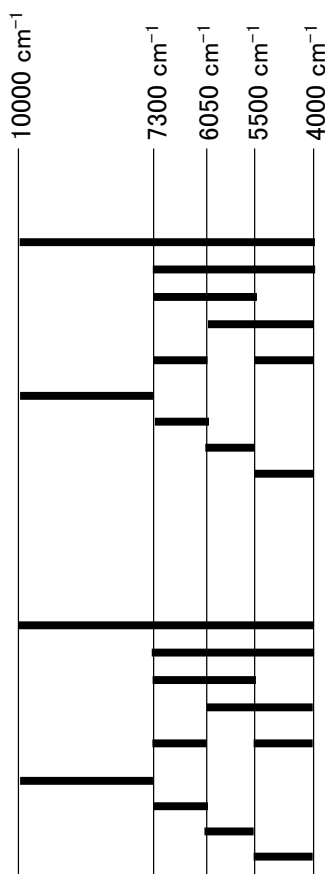
(a)

Spectral region (cm <sup>-1</sup> )	Factors	Calibration set		Prediction set		Correct prediction (%)
		$R_c^2$	RMSEC	$R_p^2$	RMSEP	
10000 – 4000	8	0.52	0.69	0.49	0.71	93.8
7300 – 4000	10	0.66	0.58	0.58	0.65	93.8
7300 – 5500	10	0.54	0.68	0.45	0.74	85.4
6050 – 4000	10	0.65	0.59	0.57	0.66	89.6
7300 – 6050	10	0.65	0.59	0.53	0.68	91.7
5500 – 4000	10	0.65	0.59	0.53	0.68	91.7
10000 – 7300	9	0.68	0.56	0.32	0.82	79.2
7300 – 6050	7	0.32	0.82	0.25	0.87	77.1
6050 – 5500	9	0.53	0.68	0.48	0.72	83.3
5500 – 4000	9	0.61	0.62	0.56	0.66	89.6

(b)

Spectral region (cm <sup>-1</sup> )	Factors	Calibration set		Prediction set		Correct prediction (%)
		$R_c^2$	RMSEC	$R_p^2$	RMSEP	
10000 – 4000	7	0.72	0.53	0.54	0.68	89.6
7300 – 4000	9	0.75	0.50	0.56	0.66	91.7
7300 – 5500	10	0.69	0.56	0.56	0.66	93.8
6050 – 4000	8	0.72	0.53	0.54	0.68	87.5
7300 – 6050	8	0.71	0.54	0.55	0.67	89.6
5500 – 4000	8	0.71	0.54	0.55	0.67	89.6
10000 – 7300	2	0.42	0.76	0.23	0.88	68.8
7300 – 6050	2	0.33	0.82	0.28	0.85	72.9
6050 – 5500	10	0.56	0.66	0.53	0.69	81.3
5500 – 4000	8	0.69	0.56	0.52	0.69	85.4





(c)

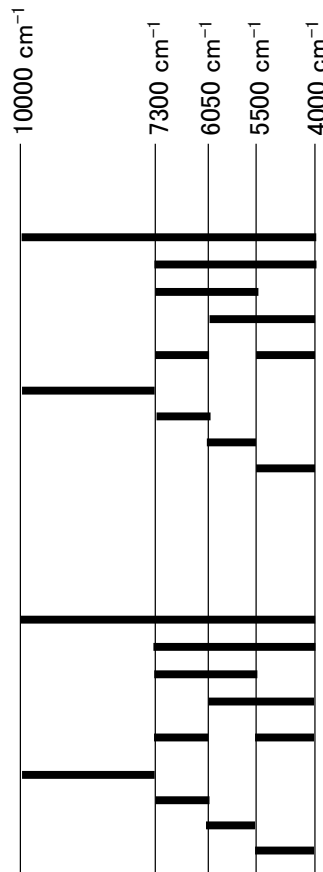
Spectral region (cm <sup>-1</sup> )	Factors	Calibration set		Prediction set		Correct prediction (%)
		$R_c^2$	RMSEC	$R_p^2$	RMSEP	
10000 – 4000	10	0.91	0.30	0.74	0.51	91.7
7300 – 4000	9	0.90	0.31	0.69	0.56	87.5
7300 – 5500	5	0.35	0.80	0.30	0.84	75.0
6050 – 4000	10	0.90	0.32	0.64	0.60	87.5
7300 – 6050	10	0.87	0.36	0.65	0.59	87.5
5500 – 4000	10	0.87	0.36	0.65	0.59	87.5
10000 – 7300	7	0.73	0.52	0.21	0.89	83.3
7300 – 6050	6	0.33	0.82	0.01	1.07	54.2
6050 – 5500	9	0.77	0.48	0.39	0.78	79.2
5500 – 4000	10	0.86	0.38	0.60	0.63	87.5

(d)

Spectral region (cm <sup>-1</sup> )	Factors	Calibration set		Prediction set		Correct prediction (%)
		$R_c^2$	RMSEC	$R_p^2$	RMSEP	
10000 – 4000	5	0.79	0.46	0.59	0.64	87.5
7300 – 4000	8	0.91	0.30	0.71	0.54	95.8
7300 – 5500	4	0.72	0.53	0.67	0.58	87.5
6050 – 4000	8	0.88	0.35	0.66	0.58	95.8
7300 – 6050	6	0.74	0.51	0.64	0.60	87.5
5500 – 4000	6	0.74	0.51	0.64	0.60	87.5
10000 – 7300	1	0.19	0.90	0.02	0.99	54.2
7300 – 6050	5	0.64	0.60	0.33	0.82	75.0
6050 – 5500	5	0.65	0.59	0.59	0.64	91.7
5500 – 4000	6	0.72	0.53	0.61	0.62	87.5

23

24



(e)

Spectral region (cm <sup>-1</sup> )	Factors	Calibration set		Prediction set		Correct prediction (%)
		$R_c^2$	RMSEC	$R_p^2$	RMSEP	
10000 – 4000	9	0.92	0.28	0.80	0.45	100
7300 – 4000	9	0.93	0.27	0.75	0.50	97.9
7300 – 5500	7	0.81	0.44	0.77	0.48	100
6050 – 4000	9	0.93	0.27	0.81	0.43	100
7300 – 6050	9	0.91	0.30	0.78	0.47	100
5500 – 4000	9	0.91	0.30	0.78	0.47	100
10000 – 7300	8	0.81	0.44	0.56	0.67	93.8
7300 – 6050	10	0.86	0.37	0.65	0.59	95.8
6050 – 5500	9	0.91	0.30	0.84	0.40	100
5500 – 4000	10	0.95	0.22	0.83	0.42	100

(f)

Spectral region (cm <sup>-1</sup> )	Factors	Calibration set		Prediction set		Correct prediction (%)
		$R_c^2$	RMSEC	$R_p^2$	RMSEP	
10000 – 4000	8	0.97	0.18	0.83	0.41	100
7300 – 4000	7	0.92	0.28	0.86	0.37	100
7300 – 5500	8	0.91	0.30	0.73	0.52	95.8
6050 – 4000	7	0.92	0.29	0.86	0.38	100
7300 – 6050	7	0.92	0.28	0.85	0.39	100
5500 – 4000	7	0.92	0.28	0.85	0.39	100
10000 – 7300	7	0.98	0.12	0.46	0.74	75.0
7300 – 6050	5	0.82	0.43	0.48	0.72	87.5
6050 – 5500	10	0.90	0.31	0.81	0.44	100
5500 – 4000	7	0.91	0.30	0.85	0.39	100

25

26

27

28

Table 3. Prediction accuracies of the wooden materials used in Chion-In temple as functions of the spectral pretreatment and spectral range. The predictions were made by employing the discriminant models based on the original and second derivative spectra of the heartwood sample for wavenumbers of 7300–4000  $\text{cm}^{-1}$ . A schematic illustration is provided on the left to show each spectral region.

